J Mater Sci (2015) 50:6359–6364
DOI 10.1007/s10853-015-9185-8

CrossMark

The study of light-emitting diode fabricated on *c*-axis patterned and flat sapphire substrate

Long Li[1] · YongZheng Fang[1] · Jun Zou[2] · Canyun Zhang[2] · Fengchao Wang[2] · Yuefeng Li[2]

Received: 2 February 2015 / Accepted: 13 June 2015 / Published online: 24 June 2015
© Springer Science+Business Media New York 2015

Abstract GaN thin films and multi-quantum wells (MQWs) were grown on the *c*-axis patterned sapphire substrates and *c*-axis flat sapphire substrates by metal organic chemical vapor deposition, respectively. The surface morphology of patterned sapphire substrate and flat sapphire substrate were measured by scanning electron microscopy. The crystal structure of GaN thin films and MQWs were measured by X-ray. The optical performance of MQWs was measured by photoluminescence spectra. The residual stress of GaN thin films was studied. GaN thin films on patterned sapphire substrate has a better crystalline quality in the [102] direction than that on flat sapphire substrate. The residual stress in MQWs on PSS is $\delta_{xx} = 1.10$ GPa, $\delta_{yy} = 0.13$ GPa, while the residual stress of films on FSS is $\delta_{xx} = 0.83$ GPa, $\delta_{yy} = 0.10$ GPa. It is found that the wavelength becomes shorter and the emission intensity becomes stronger on patterned sapphire substrate.

Introduction

GaN is widely used in the study of ultraviolet detectors, microwave devices, LED chips, and laser [1–4]. GaN-based LED is an environmental, energy saving, and long lived of the blue light-emitting devices. But these devices have not absolutely replaced other lighting devices for their low light extraction efficiency (LEE). Only a small percentage of photons escape from the LEDs and much of them eventually converts to heat. On the other hand, their light extraction efficiency is still limited by the total internal reflection at the interface. Furthermore, poor directional emission profiles of LEDs limit their application because of the broad radiation pattern from the surface and sidewalls.

Although InGaN/GaN LEDs are commercially available, the LEE is still needed for further improvement. The limitation of LEE is mainly attributed to the low internal quantum efficiency (IQE) and light extraction efficiency [5]. The low IQE results from the high threading dislocation (TD) density of GaN films grown on a hetero-substrate [6]. The TD creates a diffusion pathway for metals that electrons injected into the active layer can leak through [7].

In order to further enhance the performance of LEDs, it needed to improve the IQE and to increase their light output power. Predecessors have done a lot of work, such as the research of multiple quantum well [8], phosphors [9], fluorescence crystals [10], and flip LED [11], etc. Now many researchers have focused their study on how to obtain better crystalline quality of GaN films on the sapphire substrates [12] and how to improve the quantum efficiency [13, 14].

Low-dislocation-density GaN from single cantilever overgrowth on deep trenched sapphire substrates has been reported earlier [15]. Enhancement of the external efficiency in GaN-based LEDs grown on patterned sapphire substrates has been achieved based on the effect of the optical reflection from the side edge of the etched sapphire [16]. Chang et al. also reported that it can enhance the intensity of electroluminescence (EL) when LEDs are grown on a shallow-trenched sapphire substrate [17].

✉ Jun Zou
zoujun@sit.edu.cn

[1] School of Materials Science and Engineering, Shanghai Institute of Technology, Shanghai 201418, People's Republic of China

[2] School of Science, Shanghai Institute of Technology, Fengxian, Shanghai 201418, People's Republic of China

In this paper, the substrates (PSS) and flat sapphire substrates (FSS) were researched to enhance LEE. GaN thin films and multi-quantum wells (MQWs) were grown on PSS and FSS by metal organic chemical vapor deposition (MOCVD). The stress of GaN thin films and the special reflection of PSS were systematically studied.

Materials and methods

The sapphire substrates' diameter is 2 inches and the thickness is 430 μm, respectively. GaN thin films and MQWs were grown on the *c*-axis PSS and *c*-axis FSS by MOCVD. Trimethylgallium (TMGa), trimethylindium (TMIn), ammonia (NH_3), bis-cyclopentadienyl (Cp_2Mg), and silane (SiH_4) were used as sources of Ga, In, N, Mg, and Si.

At first, the process of GaN thin films is as follows: firstly, the GaN buffer layer were grown at a low temperature of 566 °C and the thickness is 30 nm; then the undoped GaN films were grown at a higher temperature of 1020 °C and the thickness is 2.74 μm which is the second step. Schematic diagram of GaN thin films' structure is shown in Fig. 1.

Then, the MQWs would be grown on the GaN thin films. At first, Si-doped GaN as N-type junction would be grown on undoped GaN thin films at the temperature of 995 °C, and the thickness is 2.95 μm. Secondly, GaN as the barrier with the thickness of 3 nm and InGaN as the well with the thickness of 12.7 nm would be grown on n-GaN successively at the temperature of 834 and 750 °C, respectively. This second process was repeated seven times; multi-quantum well had been created. At last, Mg-doped GaN as P-type junction would be grown. The growth process of Mg-doped GaN as P-type junction consists of two steps: Mg-doped GaN would be grown at 795 °C with the thickness of 25 nm, then Mg-doped GaN would be grown at 908.5 °C with the thickness of 70 nm. The schematic diagram of GaN-based light-emitting diodes' structure is show in Fig. 2.

PSS's surface morphology was studied by SEM (VEGA\\TESCAN type scanning electron microscope produced by TESAN company in Czech). The crystal structure of GaN thin films and MQWs was characterized by X-ray diffraction. The optical properties of LED were measured by photoluminescence (PL) (FSL920).

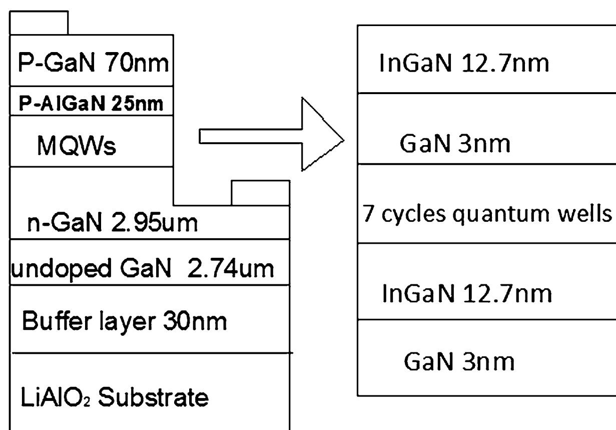

Fig. 2 Schematic diagram of GaN-based light-emitting diodes' structure

Results and discussion

The surface morphology of FSS and PSS are shown in Fig. 3. The shape of PSS with the character of the pyramid is different from Wuu [18]. The Fig. 3a, c are the plan-forms of FSS and PSS, respectively. From the Fig. 3b, FSS has a good flatness and doesn't have any impurity. The pyramid has the similar height and bottom diameter. The average height and bottom diameter are 1.71 and 2.57 μm, respectively.

The crystal structure of GaN thin films was characterized by X-ray diffraction rocking curves. Figure 4 shows the (002) and (102) orientation's X-ray rocking curves of GaN thin films on *c*-axis FSS and PSS. As shown in Fig. 4a, the full width at half maximum (FWHM) of GaN (002) plane on PSS and FSS are 0.101° and 0.102°, respectively, and the resolution of PSS and FSS are 2.3395×10^{-7} and 2.3211×10^{-7}°/a.u, respectively. While the FWHM of (102) plane are 0.103° and 0.226°, respectively, and the resolution of PSS and FSS are 5.0920×10^{-6} and 2.4210×10^{-5}°/a.u, respectively. No matter from the (002) or (102) plane, the films on PSS were better than FSS.

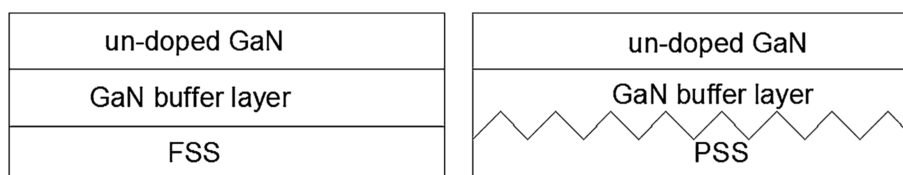

Fig. 1 Schematic diagram of GaN thin films' structure

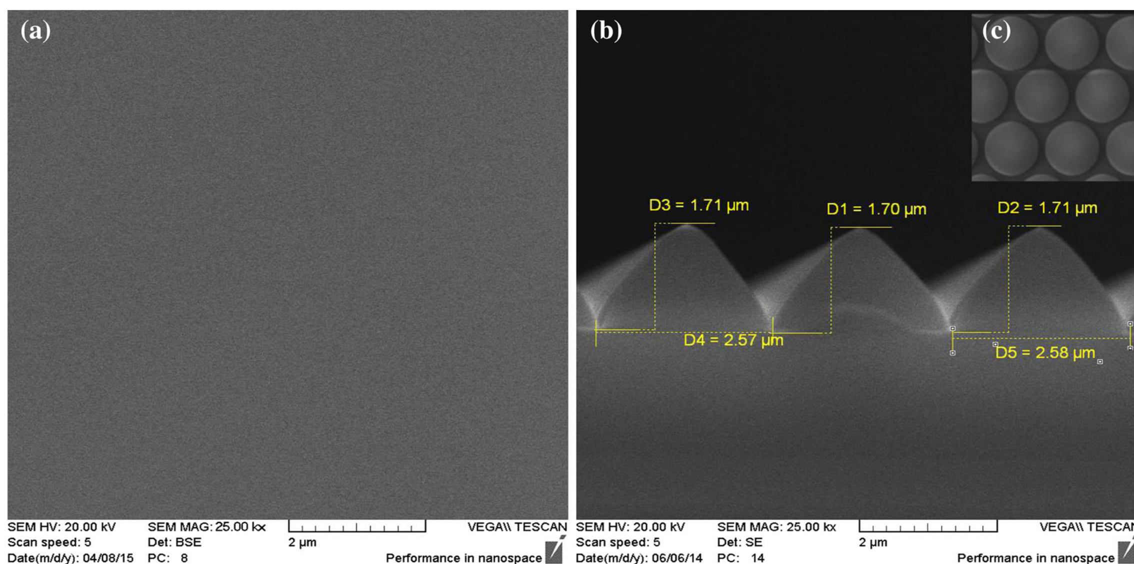

Fig. 3 SEM image of FSS and PSS

Kaganner et al. [19] have recently published a model to correlate the dislocation density from the FWHM of the peak in X-ray diffraction using reciprocal space maps. In his work, it is shown that the FWHM is proportional to $\sqrt{\rho/d}$. It is given in Eq. (1).

$$\Delta q \propto \sqrt{\rho/d} \text{or } \Delta q = k\sqrt{\rho/d}, \tag{1}$$

where Δq is value of FWHM, ρ is the dislocation density (cm^{-2}), and d is the total thickness (cm^{-2}) of the thin films on the substrate. The rough equivalent of FWHM in Fig. 4a indicates that the dislocation density of GaN thin film on both PSS and FSS is all so roughly equivalent. But the peak diffraction angle of GaN thin films on FSS is 17.048°, which is closer to the standard value 17.281° than that of films on PSS (16.902°).

As shown in Fig. 4b, it can be known that the GaN thin film's dislocation density of PSS is less than that of the FSS. But from the peak diffraction angle, the FWHM of MQWs on the PSS is 0.103° which is smaller than that on FSS (0.226°). So the MQWs on PSS has a better crystalline quality in the [102] direction than that on FSS.

The crystal structure of MQWs was studied by high-resolution X-ray diffraction (HRXRD). Figure 5 shows the HRXRD curves of MQWs on c-axis flat substrate and PSS. The strongest peak comes from the GaN. The peaks on the left side of the GaN peak come from the $In_{0.1}Ga_{0.9}N$/GaN MQWs with -1st, -2nd, -3rd, and -4th orders. The peaks on the right side of the GaN peak come from the n-AlN/n-GaN multilayer fringes of +1st, +2nd, and +3rd orders. The fourth satellite peak can be clearly observed for two samples, which indicated that the two samples have the similar smooth interface [20], so the quality of MQWs is wonderful on both substrates. It can be known that the IQE of MQWs is not very clearly improved after using PSS.

According to the Bragg equation and Hoffman [21] formula, the relationship between the stress and the diffraction angle is shown in Eqs. (2)–(9):

$$2d_{hkl}\sin\theta = n\lambda \tag{2}$$

$$\frac{1}{d_{hkl}^2} = \frac{4}{3}\frac{h^2 + hk + k^2}{a^2} + \frac{l^2}{c^2} \tag{3}$$

$$\varepsilon_{xx} = \frac{a_{\text{epi}} - a_0}{a_0} \tag{4}$$

$$\varepsilon_{yy} = \frac{m_{\text{epi}} - m_0}{m_0} \tag{5}$$

$$\varepsilon_{zz} = \frac{c_{\text{epi}} - c_0}{c_0} \tag{6}$$

$$\delta_{xx} = c_{11}.\varepsilon_{xx} + c_{12}.\varepsilon_{yy} + c_{13}.\varepsilon_{zz} \tag{7}$$

$$\delta_{yy} = c_{12}.\varepsilon_{xx} + c_{11}.\varepsilon_{yy} + c_{13}.\varepsilon_{zz} \tag{8}$$

$$\delta_{zz} = c_{13}.\varepsilon_{xx} + c_{13}.\varepsilon_{yy} + c_{33}.\varepsilon_{zz}, \tag{9}$$

where $X\|[11\bar{2}0]$ GaN, $Y\|[1\bar{1}00]$ GaN, $Z\|[0001]$ GaN, ε_{xx} represents X direction's strain epsilon, ε_{yy} represents Y direction's strain epsilon, ε_{zz} represents Z direction's strain epsilon. δ_{xx} represents X direction's residual stress, δ_{yy} represents Y direction's residual stress, δ_{zz} represents Z direction's residual stress. In the Eqs. (7)–(9): $c_{11} = 3.9 \times 10^{11}$ N/m^2, $c_{12} = 1.45 \times 10^{11}$ N/m^2, $c_{13} = 1.06 \times 10^{11}$ N/m^2, $c_{33} = 3.98 \times 10^{11}$ N/m^2, and the [0001] plane $\delta_{zz} = 0$.

According to the above equations, the residual stress of GaN thin films can be calculated which is shown in Table 1.

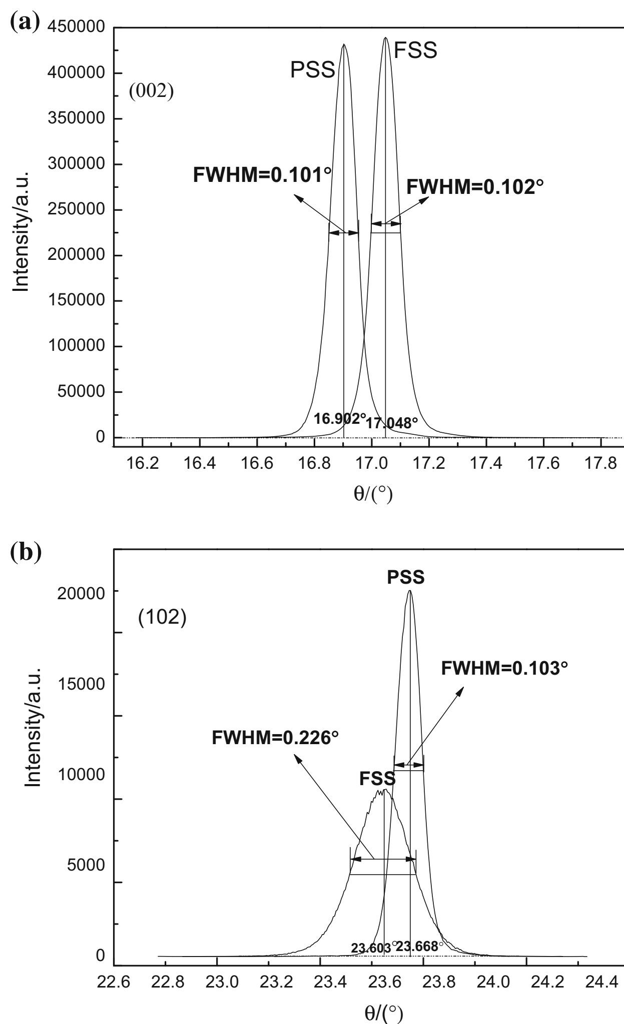

Fig. 4 The double crystal X-ray rocking curves for symmetric (002) and (102) plane of GaN thin films on PSS and FSS

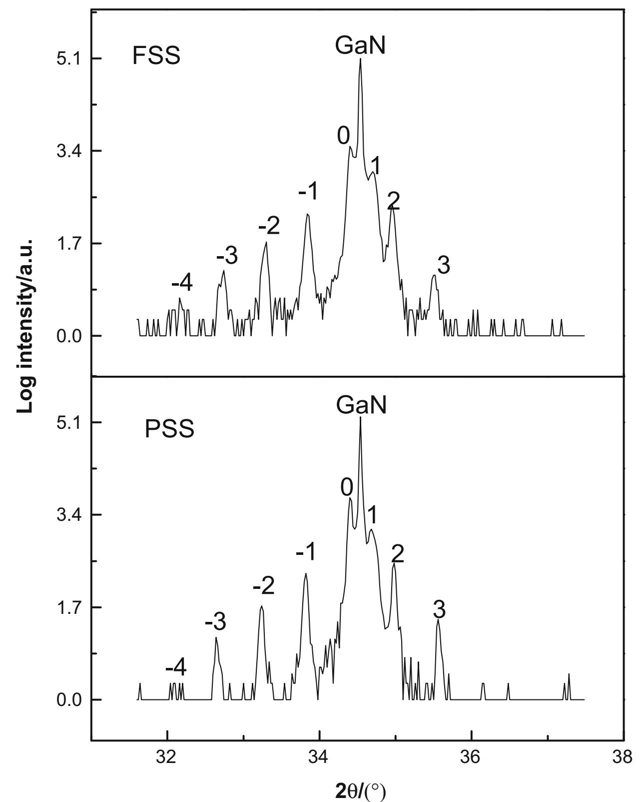

Fig. 5 Measured HRXRD curves and simulation for c flat plane and PSS substrates

In the Table 1, the negative value represents residual stress. So the residual stress of GaN thin films on PSS and FSS are compressive stress. Meanwhile, the stress in GaN thin films on PSS is larger than that on FSS. The cell volume of the GaN is: $V = a^2 \cdot c \cdot \sin 120°$, the values of PSS and FSS are 45.407 and 45.473 Å^3, respectively. The values of FSS are larger than PSS, so the LED on the PSS would have higher density of electrons and holes. The stress in the GaN films on the PSS: $\delta_{xx} = -1.098$ GPa, $\delta_{yy} = -0.132$ GPa; FSS: $\delta_{xx} = -0.827$ GPa, $\delta_{yy} = -0.100$ GPa. The films on PSS had subjected to larger stress in the *X* and *Y* direction than FSS.

Therefore the density of electrons and holes in GaN thin films on PSS is higher too, the intensity of carrier diffusion becomes powerful, and thus the depletion layer becomes broad, so the band gap becomes larger. All of these maybe resulted in MQWs on PSS having a shorter wavelength and stronger luminous intensity compared to that on FSS. It can be confirmed by PL spectra of MQWs.

Table 2 gives the data of PL spectra to measure the optical performance of MQWs on PSS and FSS. In the Table 2, AVR represents the average, and STD represents the standard deviation. As we all know, the higher the luminous intensity, the better is the quality of MQWs, and also the higher is the light extraction efficiency. It is observed that the light intensity of MQWs on PSS is 4836.96 and that on FSS is 718.60 from Table 2; the light intensity of MQWs on PSS is almost seven times of that on FSS. Therefore the light extraction efficiency of MQWs is improved after using PSS. On the other hand, the peak wavelength and dominant wave of GaN-based light-emitting diodes on PSS are 447.22 and 452.47 nm, respectively while the peak wavelength and dominant wave of GaN-based light-emitting diodes on FSS are 466.58 and 469.79 nm, respectively. It means that the wavelength of GaN-based light-emitting diodes on PSS appeals blue shift compared to that on the FSS, which is consistent to XRD results in Fig. 4a.

On one hand, compressive stress is contributed to increase the luminous intensity on PSS, because higher density of electrons and holes would lead to larger amount of photons as a result of the recombination of electrons and holes. On the other hand, the increase of luminous intensity

Table 1 The residual stress of GaN thin films

	ε_{xx} (10^{-3})	ε_{yy} (10^{-4})	ε_{zz} (10^{-4})	δ_{xx} (GPa)	δ_{yy} (GPa)	a (Å)	c (Å)
FSS	−2.452	5.157	5.157	−0.827	−0.100	3.181	5.189
PSS	−3.258	6.849	6.849	−1.098	−0.132	3.179	5.190

Table 2 The data of PL spectra of MQWs

	Peak wavelength		Dominant wave		FWHM		PL intensity		Intergrated int		Reflectance	
	AVR	STD	AVR	STD	AVR	STD	AVR	STD	AVR	STD	AVR	STD
PSS	447.22	2.07	452.47	1.67	18.87	0.64	4836.96	423.59	120304.11	7312.61	220.39	2.11
Flat	466.58	2.65	469.79	2.05	21.75	1.04	718.60	81.62	20463.24	2170.71	234.87	2.22

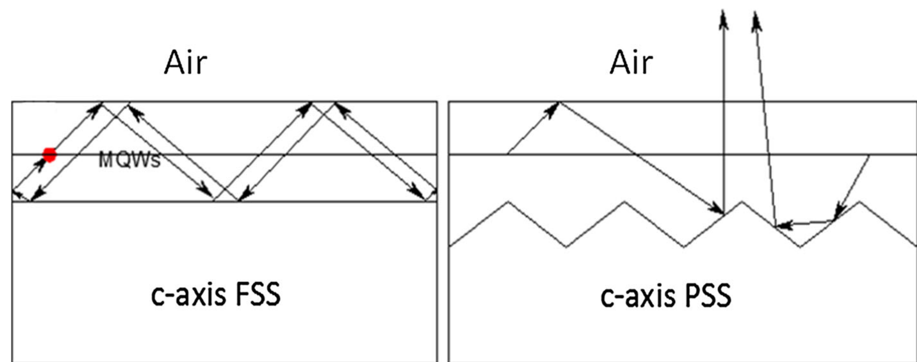

Fig. 6 The reflection system of PSS and FSS

is also related with the special reflection system of PSS. Figure 6 is the reflection system of PSS and FSS.

The refractive index of GaN layer, sapphire, and air are about 2.4, 1.7, and 1.0, respectively. From Fig. 6, the light easily occurs because the GaN surface is paralleled to the substrates (FSS), and the angle of total reflection is smaller than 25° ($\sin\theta = n_1/n_2$). Much of the light can't reflect out from GaN surface, so the luminous intensity is lower. While the light propagation direction is changed uncertain for the GaN surface, it isn't parallel to the substrates on the PSS obviously. So more photons would reflect out to the air, and it improved the light extracting efficiency of GaN-based LED on PSS.

Conclusion

GaN thin films and InGaN/GaN MQWs LEDs were grown by MOCVD. The residual stress of GaN thin films on PSS is $\delta_{xx} = -1.098$ GPa, $\delta_{yy} = -0.132$ GPa, the residual stress of GaN thin films on FSS is $\delta_{xx} = -0.827$ GPa, $\delta_{yy} = -0.100$ GPa. The residual stress is compressive stress, it results in the wavelength on PSS appeals blue shift compared the FSS, and IQE haven't improved after used PSS. The compressive stress, special reflection system, and the better crystalline quality in the (102) plane of MQWs on PSS are contributed to its higher luminous intensity.

Acknowledgements This work was supported by the National Natural Science Foundation of China (Grant No. 51302171), Shanghai Institute of Technology Talents Scheme (Grant No. YJ2014-04), Shanghai-disciplinary capacity building projects (Grant No. 14500503300), Shanghai Alliance Program (Grant No. Lm201318), Shanghai Cooperative Project (Grant No. ShanghaiCXY-2013-61), Jiashan County Technology Program (Grant No. 20141316), and Shanghai Natural Science Foundation (Grant No. 12ZR1430900).

References

1. Przeździecka E, Gościński K, Stachowicz M, Dobosz D, Zielony E, Sajkowski JM, Pietrzyk MA, Płaczek-Popko E, Kozanecki A (2013) Spectrum selective UV detectors from an p-ZnO:As/n-GaN diodes grown by Molecular Beam Thin films. Sens Actuator A 195:27–31
2. Crupi G, Avolio G, Raffo A, Barmuta P, Dominique M, Schreurs MP, Caddemi A, Vannini G (2011) Investigation on the thermal behavior of microwave GaN HEMTs. Solid State Electron 64:28–33
3. Zhuo XJ, Zhang J, Li DW, Wang XF, Wang WL, Diao JS, Li K, Yu L, Zhang YW, Li ST (2014) Enhanced performances of InGaN/GaN-based blue LED with an ultra-thin inserting layer between GaN barriers and InGaN wells. Opt Commun 325:129–133
4. Alahyarizadeh G, Hassan Z, Thahab SM, Yam FK, Ghazai AJ (2014) Performance characteristics of deep violet InGaN DQW

laser diodes with InGaN/GaN superlattice waveguide layers. Optik 125:341–344
5. Cuong TV, Cheong HS, Kim HG, Kim HY, Hong CH, Suh EK, Cho HK, Kong BH (2007) Enhanced light output from aligned micropit InGaN-based light emitting diodes using wet-etch sapphire patterning. Appl Phys Lett 90:131107–131109
6. Watanabe S, Yamada N, Nagashima M, Ueki Y, Sasaki C, Yamada Y, Taguchi T, Tadatomo K, Okagawa H, Kudo H (2003) Internal quantum efficiency of highly-efficient $In_xGa_{1-x}N$-based near-ultraviolet light-emitting diodes. Appl Phys Lett 83:4906–4908
7. Hsu CY, Lan WH, Wu YCS (2003) Effect of thermal annealing of Ni/Au ohmic contact on the leakage current of GaN based light emitting diodes. Appl Phys Lett 83:2447–2449
8. Asghar M, Hurwitz E, Melton A, Jamil M, Ferguson IT, Tsu R (2012) Investigation of electron energy states in InGaN/GaN multiple quantum wells. Phys B 407:2850–2853
9. Park JY, Lee JH, Raju GSR, Moon BK, Jeong JH, Choi BCh, Kim JH (2014) Synthesis and luminescent characteristics of yellow emitting GdSr2AlO5:Ce^{3+} phosphor for blue light based white LED. Ceram Int 40:5693–5698
10. Tang L, Xia HP, Wang PY, Peng JT, Zhang YP, Jiang HC, Chen HB (2014) White light emission from Eu^{3+}/Dy^{3+} Co-doped LiYF4 crystal excited by UV light. Mater Lett 104:37–40
11. Lachab M, Asif F, Zhang B, Ahmad I, Heidari A, Fareed Q, Adivarahan V, Khan A (2013) Enhancement of light extraction efficiency in sub-300 nm nitride thin-film flip-chip light-emitting diodes. Solid State Electron 89:156–160
12. Son JS, Honda Y, Yamaguchi M, Amano H, Baik KH, Seo YG, Hwang SM (2013) Characteristics of a-plane GaN films grown on optimized silicon-dioxide-patterned r-plane sapphire substratess. Thin Solid Films 546:108–113
13. Park CG, Gu GH, Lee BH, Jang DH (2013) Effects of growth pressure on the structural and optical properties of multi quantum wells (MQWs) in blue LED. Ultramicroscopy 127:114–118
14. Wang JC, Fang CH, Wu YF, Chen WJ, Kuo DC, Fan PL, Jiang JA, Nee TE (2012) The effect of junction temperature on the optoelectrical properties of InGaN/GaN multiple quantum well light-emitting diodes. J Lumin 132:429–433
15. Ashby CIH, Mitchell CC, Han J, Missert NA, Provencio PP, Follstaedt DM, Peake GM, Griego L (2000) Low-dislocation-density GaN from a single growth on a textured substrate. Appl Phys Lett 77:3233–3235
16. Yamada M, Mitani T, Narukawa Y, Shioji S, Niki I, Sonobe S, Deguchi K, Sano M, Mukai T (2002) InGaN-based near-ultraviolet and blue-light-emitting diodes with high external quantum efficiency using a patterned sapphire substrate and a mesh electrode. Jpn J Appl Phys 41:1431–1433
17. Chang SJ, Lin YC, Su YK, Chang CS, Wen TC, Shei SC, Ke JC, Kuo CW, Chen SC, Liu CH (2003) Nitride-based LEDs fabricated on patterned sapphire substrates. Solid State Electron 47:1539–1542
18. Wuu DS, Wang WK, Shih WC, Horng RH, Lee CE, Lin WY, Fang JS (2005) Enhanced output power of near-ultraviolet InGaN–GaN LEDs grown on patterned sapphire substrates. IEE Photonic Technol Lett 17:288–290
19. Kaganer VM, Köhler R, Schmidbauer M, Opitz R (1997) X-ray diffraction peaks due to misfit dislocations in heteroepitaxial structures. Phys Rev B 55:1709–1810
20. Gao H, Yan F, Zhang Y, Li JM, Zeng YP, Wang GH (2008) Enhancement of the light output power of InGaN/GaN light-emitting diodes grown on pyramidal patterned sapphire substrates in the micro-and nanoscale. J Appl Phys 103:14314
21. Hoffman RW (1976) Physics of Nonmetallic Thin Films. In: Hoffman RW (ed) Mechantcal properties of non-metallic thin films, 1st edn. Plenum, New York, pp 273–353